

- (41) Lee, K. J.; Eichinger, B. E. *Macromolecules* 1989, 22, 1441.
(42) Dusek, K. In *Developments in Polymerization*; Harward, R. N., Ed.; Applied Science: Barking, U.K., 1982; Vol. 3.
(43) Flory, P. J. *Macromolecules* 1982, 15, 99.
(44) Antonietti, M.; Fölsch, K. J.; Sillescu, H.; Pakula, T. *Macromolecules* 1989, 22, 2812.
Registry No. (Styrene)(*m*-DIB) (copolymer), 26124-82-3.

Effect of Surrounding Medium on Intramolecular Conformational Changes in Probe Molecules

Ivet Bahar* and Burak Erman

Polymer Research Center and School of Engineering, Bogazici University, Bebek 80815, Istanbul, Turkey

Lucien Monnerie

Laboratoire de Physicochimie Structurale et Macromoléculaire, associé au CNRS, ESPCI, 10 rue Vauquelin, 75231 Paris, France

Received November 13, 1989; Revised Manuscript Received February 12, 1990

ABSTRACT: Conformational dynamics of short probes dispersed in a matrix is investigated. The matrix can be in two states, fast or slow, depending on the amount of free volume. Following the work of Anderson and Ullman,⁴ the amount of free volume is assumed to fluctuate in time, thus modifying the states of the matrix. The probe undergoes transitions between two states resembling trans-cis isomeric transitions. Correlation times of the probe-matrix system exhibit a clear transition as the free-volume fluctuations of the matrix become faster. In a fast matrix, the temperature dependence of correlation times for probes reflects both the intramolecular conformational barrier in the probe and the energy change of viscous origin in the matrix, while in a slow matrix only the activation energy of the matrix is observed. This is in agreement with the results from recent experiments with fluorescent probes dissolved in small-molecule solvents and in bulk polymer.

Introduction

Intramolecular excimer formation in fluorescent probe molecules has been shown to give information about the dynamics of the environment in which they are dispersed in small quantities.¹ A large body of experimental work confirms the efficiency of this technique in understanding the dynamics of various size molecules, ranging from small solvent molecules to polymers in the bulk state.

In general, the internal reorientation of the probe is opposed both by intramolecular conformational barriers and by intermolecular resistance of viscous origin. In fact, in a matrix of small or oligomeric molecules, the activation energy for the motion of the probe is observed from experiments to be equal to the sum of (i) the activation energy for intramolecular rotameric transitions of the probe and (ii) the one associated with the viscosity of the environment.² For probes dispersed in a bulk polymer, however, the temperature dependence of the probe motion is characteristic of the surrounding medium only; i.e., the mobility of the bulk polymer is the factor almost totally controlling the motion of the probe. The specific aim of the present paper is to investigate, theoretically, the cause of this change in the observed activation energies or in the extent of probe-matrix coupling depending on the mobility of the surroundings.

A first description of a coupling of this nature is given by the defect diffusion model of Glarum.³ The model describes the cooperativity between an orienting molecule and its environment. The orientation of the molecule is more likely immediately after one of its neighbors relaxes. The relaxing neighbor is treated as a defect that may

diffuse toward the reorienting molecule. The diffusion coefficient associated with the motion of the defect describes the mobility of the environment. The defect diffusion model was further explored, in a more refined way, by Anderson and Ullman.⁴ According to this model, the environment about each molecule is taken to fluctuate with time. These fluctuations are assumed to critically affect the reorientation probabilities of the molecule. The fluctuations of the environment are associated with fluctuations of free volume. The work of Anderson and Ullman is the first rigorous attempt in establishing the dynamic nature of the free-volume effect in intermolecular correlations. The concept of a fluctuating environment was further treated by Anderson⁵ in terms of a "simple defect" model. According to this model, the environment of a given molecule can be in either of two states. One of the states is "unyielding". A molecule in this state has a small probability of reorientation. The second state constitutes a defect in which the molecule has a high probability of reorienting. The motion of the molecule may in its most general form be described in terms of the well-known Ornstein-Uhlenbeck process as shown by Anderson and Ullman. A similar treatment has been employed by Sillescu⁶ as well, in describing magnetic spin resonance line shapes in liquids with molecular reorientation. In the present study, we reconsider the dynamics of a probe molecule by solving the master equation for a rotational jump model in which the rates of internal transitions of the probe molecule depend on the state of its immediate surrounding. The formulation though less formal than that of Anderson-Ullman and Sillescu helps for a clear

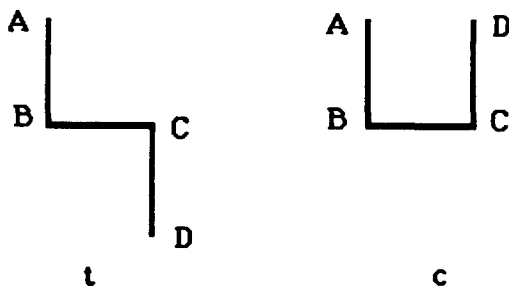


Figure 1. Schematic representation of the isomeric states *t* and *c* for a central bond BC in a probe molecule.

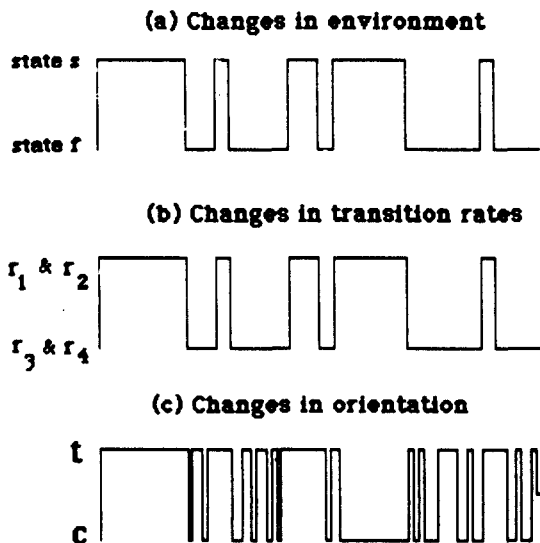


Figure 2. Hypothetical sequence of isomeric transitions (part c) coupled to the changes in environment (part a). Part b shows the transition rate constants prevailing in the slow and fast environments.

understanding of probe-matrix coupling behavior in general.

The Model and Basic Assumptions

In the interest of simplifying the discussion, we first investigate the internal dynamics of a two-state bond and its coupling with the environment, which we call the matrix. The bond in question belongs to a probe molecule, which undergoes conformational transitions. Such transitions are responsible for experimentally observable responses such as excimer emission following the excitation of a bi-chromophoric molecule. In Figure 1, two states of an investigated central bond BC are shown. Depending on the isomeric state of bond BC, the relative position and orientation of the adjacent bonds AB and CD change. The state resembling the trans state of a real bond will be called the *t* state, and the one resembling the cis state will be called the *c* state.

Following the work of Anderson,⁵ the surroundings are assumed to exist in two distinct states, which we refer to as the fast (*f*) and the slow (*s*) states. The term surroundings is employed in a restricted sense to indicate the near neighborhood of the probe or of the associated moving sequence. The rates of isomeric transitions are affected by the state of the surroundings. The forward and reverse passages from *t* to *c* are governed by the respective rate constants r_1 and r_2 in the slow environment and by r_3 and r_4 in the fast environment. A clear scheme described by Anderson is shown in Figure 2. Parts a and b in the figure illustrate the change with time in the environment of probe and in the prevailing rate constants.

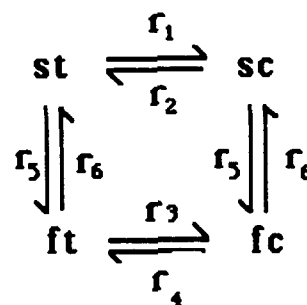


Figure 3. Kinetic scheme for the transitions between the joint states *st*, *sc*, *ft*, and *fc*. Here *s* and *f* refer to the slow and fast states of the matrix.

The accompanying reorientation of the probe is shown in part c. The latter corresponds to the extreme case where the reorientation is presumed impossible whenever the probe is in the slow (*s*) environment. To keep the generality, we will assume that conformational transitions are possible in the slow environment; i.e., r_1 and r_2 are different from zero. However, bearing in mind that the probe reorientation is possible only if sufficient free volume is supplied by the surroundings, the rate constants r_1 and r_2 of conformational transitions in the slow medium are assumed to be bounded above by the rate of fluctuations of free volume in the matrix. The latter are represented by the rate constants r_5 and r_6 of passages between the fast and slow states.

For the two-state bond and the two-state matrix system, the dynamics may be described in terms of transitions among the four joint states, *st*, *sc*, *ft*, and *fc*. A schematic description of these transitions is shown in Figure 3, where the various r_i denote the rate constants associated with the transitions between the four states. No transition is assumed to take place between the *sc* and *ft* states and *st* and *fc* states. The transitions between slow and fast matrices (r_5, r_6) are taken to be independent of the states of the bond, based on the assumption⁴ that the fluctuations of the matrix are independent of the conformational transitions of the probe. For stationary systems where the principle of detailed balance holds, we have

$$r_5/r_6 = p_{fc}/p_{sc} = p_{ft}/p_{st} \quad (1)$$

where p_{fc} , p_{ft} , p_{sc} , and p_{st} are the equilibrium probabilities of the states *fc*, *ft*, *sc*, and *st*, respectively. Similar identities of the form

$$\begin{aligned} r_1/r_2 &= p_{sc}/p_{st} \\ r_3/r_4 &= p_{fc}/p_{ft} \end{aligned} \quad (2)$$

may be written for the rotameric transitions. The eqs 1 and 2 imply that

$$r_1/r_2 = r_3/r_4 = p_c/p_t \quad (3)$$

where the equilibrium probabilities p_t and p_c for the *t* and *c* states are given by

$$\begin{aligned} p_t &= p_{ft} + p_{st} \\ p_c &= p_{fc} + p_{sc} \end{aligned} \quad (4)$$

Equation 3 states that the conformational probabilities for the probe remain unaffected by the environment. The forward and reverse rates between *t* and *c* states preserve the same ratio in different media, but their absolute values are modified depending on the state (*s, f*) of the matrix. The coupling with the matrix, if any, will be in the direction of slowing down of the rates of conformational transitions that would occur in the absence of environmental effects. In the limit of negligibly small environmental resistance,

i.e., very fast matrix, r_3 and r_4 assume their maximum values dictated by the probe conformational energetics.

The consideration of the joint statistics of the bond-matrix system and the identification of the different states of the matrix leads to a more detailed description of the orientational dynamics of the bonds compared to the previous work⁷ in which a mean-field approach, inherently present in Kramers' rate type expression,⁸ was adopted for the effect of the environment on the isomeric transition rates.

Extension of the present discussion to the case of a larger number of reorienting bonds is straightforward, as shown in the Appendix. Also, the theory may be adapted to more than two states accessible to the bond and to the matrix by suitable redefinition of the kinetic scheme of the model.

Rate Constants. The rate constants associated with the probe isomeric rotations are suitably described by the Kramers' expression in a high-friction medium⁸

$$r = \frac{(\gamma\gamma^*)^{1/2}}{2\pi\zeta s^2} \exp(-E/RT) \quad (5)$$

where γ and γ^* are the curvatures of the rotational energy surface at the minima and maxima, ζ is the friction coefficient, and E is the energy to be surmounted in going from one rotational state to the other. s^2 represents the sum of the squares of the paths travelled by the atoms of the molecule during the transition. In probes where the transition takes place over a single bond, s^2 may be chosen as a coefficient of proportionality. In probes exhibiting transitions over more than one bond, s^2 may take different values for each transition.

The coefficient of friction may be related to the free volume by an expression analogous to the one proposed by Doolittle for the viscosity⁹

$$\ln \zeta/kT = \ln \zeta^\circ/kT - \bar{\gamma}(1 - 1/f) \quad (6)$$

where f is the fractional free volume and $\bar{\gamma}$ and ζ° are parameters. The substitution of eq 6 into eq 5 leads to a rate expression written as the product of an intermolecular and an intramolecular term

$$r = (K_0/\zeta^\circ) \exp(-E/RT) \exp[\bar{\gamma}(1 - 1/f)] \quad (7)$$

where

$$K_0 \equiv (\gamma\gamma^*)^{1/2}/(2\pi s^2) \quad (8)$$

Inasmuch as the free volume may be regarded as a fluctuating quantity,⁴ we can assign to the slow and fast environments different values for ζ° and f depending on the local free volume. We have

$$\begin{aligned} r_1 &= K_0 g_s \exp(-E_{ct}/RT) \\ r_2 &= K_0 g_s \exp(-E_{tc}/RT) \\ r_3 &= K_0 g_f \exp(-E_{ct}/RT) \\ r_4 &= K_0 g_f \exp(-E_{tc}/RT) \end{aligned} \quad (9)$$

where

$$g_i = (1/\zeta_i^\circ) \exp[\bar{\gamma}(1 - 1/f_i)] \quad (10)$$

with $i = f$ or s for the slow or fast environments, respectively. Here, E_{ij} is the intramolecular conformational barrier for the passage from state j to state i . Also, the diffusive motion of the environment from fast to slow regime or vice versa will be described by the rate constants r_5 and r_6 . If the simple defect model of Anderson is adopted, r_5 will obey the proportionality $r_5 \sim \bar{g}$ where \bar{g} is given by eq 10 with the mean fractional free volume, \bar{f} ,

replacing f_i . As a first approximation one may assume a linear increase of \bar{f} with temperature; i.e.

$$\bar{f} = f_0 + \alpha_f(T - T_0) \quad (11)$$

where f_0 is the fractional free volume at the reference temperature, T_0 , and α_f is the thermal expansion coefficient of the fractional free volume. Equations 10 and 11 may be combined in $r_5 \sim \bar{g}$ to yield

$$r_5(T) \sim \exp\left[\frac{\bar{A}_1 \bar{A}_2}{\bar{A}_2 + (T - T_0)}\right] \quad (12)$$

which may be rearranged as

$$r_5(T) \sim \exp\left[\frac{\bar{A}_1(T - T_0)}{\bar{A}_2 + (T - T_0)}\right] \quad (13)$$

with $\bar{A}_1 = \bar{\gamma}/f_0$ and $\bar{A}_2 = f_0/\alpha_f$. Equation 12 is in form identical with the Vogel-Fulcher-Tamman equation, whereas eq 13 is in form identical with the WLF equation. The same relationship applies for r_6 .

Orientalional Dynamics. The probabilities of the four states are denoted by the vector $\mathbf{P}(t)$ given by

$$\mathbf{P}(t) = \text{col} [p_{st}, p_{sc}, p_{ft}, p_{fc}] \quad (14)$$

where col denotes column. The time evolution of $\mathbf{P}(t)$ follows the master equation

$$d\mathbf{P}(t)/dt = \mathbf{A} \mathbf{P}(t) \quad (15)$$

where the transition rate matrix \mathbf{A} for the system may be obtained from the kinetic scheme of Figure 3 as

$$\mathbf{A} = \begin{array}{c} \begin{array}{cccc} & \begin{array}{c} st \\ sc \\ ft \\ fc \end{array} & \begin{array}{c} st \\ sc \\ ft \\ fc \end{array} & \begin{array}{c} st \\ sc \\ ft \\ fc \end{array} & \begin{array}{c} st \\ sc \\ ft \\ fc \end{array} \\ \begin{array}{c} st \\ sc \\ ft \\ fc \end{array} & \begin{bmatrix} -(r_1+r_5) & r_2 & r_6 & 0 \\ r_1 & -(r_2+r_5) & 0 & r_6 \\ r_5 & 0 & -(r_3+r_6) & r_4 \\ 0 & r_5 & r_3 & -(r_4+r_6) \end{bmatrix} & & \end{array} \end{array} \quad (16)$$

The ij th element ($i \neq j$) of \mathbf{A} is the rate constant for the transition from the j th state to the i th state. For clarity, the four states are indicated above and on the left of the matrix. Each diagonal element in \mathbf{A} is equal to the negative sum of the remaining elements in the corresponding column.

The time-dependent joint probability matrix $\mathbf{P}(t)$ is obtained from the solution of eq 15 as⁷

$$\mathbf{P}(t) = \mathbf{B} \exp(\Lambda t) \mathbf{B}^{-1} \mathbf{P}(t=0) \quad (17)$$

where \mathbf{B} is the matrix of eigenvectors of \mathbf{A} , \mathbf{B}^{-1} is its inverse, Λ is the diagonal matrix of eigenvalues of \mathbf{A} , and $\mathbf{P}(t=0)$ is the vector of initial probabilities, $P_i(0)$, for state i , $i = 1-4$. For a system where the various probabilities $P_i(0)$ are not appreciably perturbed by the measurement technique, initial probabilities may be equated to the equilibrium probabilities.

The four eigenvalues of \mathbf{A} are

$$\begin{aligned} \lambda_1 &= 0 \\ \lambda_2 &= -(r_5 + r_6) \\ \lambda_3 &= -\alpha + (\alpha^2 - \beta)^{1/2} \\ \lambda_4 &= -\alpha - (\alpha^2 - \beta)^{1/2} \end{aligned} \quad (18)$$

where

$$\alpha = (1/2) \sum_{k=1}^6 r_k$$

$$\beta = (r_1 + r_2)(r_3 + r_4) + (r_1 + r_2)r_6 + (r_3 + r_4)r_5 \quad (19)$$

The zero eigenvalue specifies the equilibrium state of the system. The second eigenvalue reflects the dynamics of the matrix only. λ_3 and λ_4 represent the coupling between the bond and the matrix.

The elements of \mathbf{B} may be generated from the following relations

$$\begin{aligned} B_{1i} &= 1 \\ B_{2i} &= \frac{\lambda_i^2 + (r_1 + r_3 + r_5 + r_6)\lambda_i + r_1r_4 + r_1r_3 + r_1r_6 + r_3r_5}{(r_2 + r_4)\lambda_i + r_2r_4 + r_4r_5 + r_2r_3 + r_2r_6} \\ B_{3i} &= (r_1 + r_5 + \lambda_i - r_2B_{2i})/r_6 \\ B_{4i} &= [-r_1 + (r_2 + r_5 + \lambda_i)B_{2i}]/r_6 \end{aligned} \quad (20)$$

The elements of \mathbf{B}^{-1} are obtained from

$$[B^{-1}]_{ij} = X_{ij}/Z_i \quad (21)$$

where

$$\begin{aligned} X_{i1} &= 1 \\ X_{i2} &= \frac{\lambda_i^2 + (r_1 + r_3 + r_5 + r_6)\lambda_i + r_1r_3 + r_1r_6 + r_3r_5 + r_2r_3}{(r_1 + r_3)\lambda_i + r_1r_3 + r_1r_6 + r_2r_3 + r_3r_5} \\ X_{i3} &= (r_1 + r_5 + \lambda_i - r_1X_{i2})/r_5 \\ X_{i4} &= [-r_2 + (r_2 + r_5 + \lambda_i)X_{i2}]/r_5 \end{aligned} \quad (22)$$

and

$$Z_i = 1 + \sum_{k=2}^4 X_{ik}B_{ki} \quad (23)$$

The variables i and j in eqs 20–23 take values from 1 to 4.

For the system under consideration, the autocorrelation function, $\langle f(t) \rangle$, for a configuration-dependent variable f_{ij} associated with the transition from the j th to the i th state, is expressed as

$$\langle f(t) \rangle = \sum_{n=1}^4 k_n \exp\{-\lambda_n t\} \quad (24)$$

where

$$k_n = \sum_{j=1}^4 \sum_{i=1}^4 B_{in}[B^{-1}]_{nj} P_n(0) f_{ij} \quad (25)$$

The correlation time, τ , for $\langle f(t) \rangle$ is defined as the normalized area between the time decay curve for $\langle f(t) \rangle$ and the asymptotic value k_1 to which it converges at long times. Thus following the definition

$$\tau = \int_0^\infty [\langle f(t) \rangle - f(\infty)] / [\langle f(0) \rangle - f(\infty)] dt \quad (26)$$

we obtain by using eqs 24 and 18

$$\tau = \frac{1}{1 - k_1} \left[\frac{k_2}{r_5 + r_6} + \frac{k_3}{\alpha - (\alpha^2 - \beta)^{1/2}} + \frac{k_4}{\alpha + (\alpha^2 - \beta)^{1/2}} \right] \quad (27)$$

The first term in brackets in eq 27 contains rates for the environment or matrix only. For a property f_{ij} , which is a function of the conformational states (t,c) of the observed probe, regardless of the states (f,s) of the matrix, k_2 will equate to zero and the independent contribution of the environment to local chain dynamics will vanish. Only the last two terms in eq 27, representing the coupling of the probe to the matrix, will be operative.

The two limiting cases where the matrix is very slow and very fast compared to the intramolecular transition rates r_3 and r_4 are of special interest. For simplicity, let us take $r_5 = r_6$ in both cases.

(i) For the very fast matrix, with the inequality $r_5 \gg r_3, r_4$, the correlation time given by eq 27 reduces to

$$\tau = \frac{1}{1 - k_1} \left[\frac{2k_3}{r_1 + r_2 + r_3 + r_4} \right] \quad (28)$$

which may be further simplified as

$$\tau = \frac{1}{1 - k_1} \left[\frac{2k_3}{r_3 + r_4} \right] \quad (29)$$

for $r_1, r_2 \ll r_3, r_4$.

(ii) For the very slow matrix, the inequality $r_5 \ll r_3, r_4$ implies that

$$\tau = \frac{1}{1 - k_1} \left[\frac{k_3}{r_1 + r_2 + r_5} + \frac{k_4}{r_3 + r_4} \right] \quad (30)$$

which automatically reduces to

$$\tau = \frac{1}{1 - k_1} \left[\frac{k_3}{r_1 + r_2 + r_5} \right] \quad (31)$$

since $r_1, r_2 \leq r_5$, following the assumption delineated in the model. Further slowing down of free-volume fluctuations in a slow environment limits both r_1 and r_2 such that initially $\max(r_1, r_2)$ and subsequently both of them necessarily equate to r_5 . In this extreme case of the exclusively diffusion-controlled regime, the correlation time reads

$$\tau = \frac{1}{1 - k_1} \left[\frac{k_3}{3r_5} \right] \quad (32)$$

The resulting equalities 28–32 deserve special attention. In the fast matrix limit, the prevailing rate of conformational transition is the one dictated by the probe intramolecular energetics, mainly. The mobility of the matrix does not explicitly appear in the observed correlation time (eq 29). This is expected inasmuch as a fast matrix is identified as a near neighborhood, which accommodates the new orientation of the probe without significant slowing down of the conformational kinetics. This limiting case is representative of the internal dynamics of the single-probe small-molecule environment. However, eqs 31 and 32 show that the mobility of the surroundings becomes an increasingly important variable prescribing the correlation time when the process of reorientation within the matrix is slowed down, as in the case of the probes dispersed in bulk polymer.

For cases intermediate between very fast and very slow matrices, the expression given by eq 27 shows the joint contribution of the matrix and the probe to the observed dynamics.

Numerical Example. Orientational Autocorrelation Function (OACF). As a numerical example we study the relaxation of the first orientational autocorrelation function, $M_1(t)$ defined as

$$M_1(t) = \langle \mathbf{m}(t) \cdot \mathbf{m}(0) \rangle \quad (33)$$

where \mathbf{m} is a unit vector under consideration, the arguments t and 0 denoting the time of observation. For the simple model shown in Figure 1, with the vector \mathbf{m} along the bond CD, the term f_{ij} in eq 25 may be identified

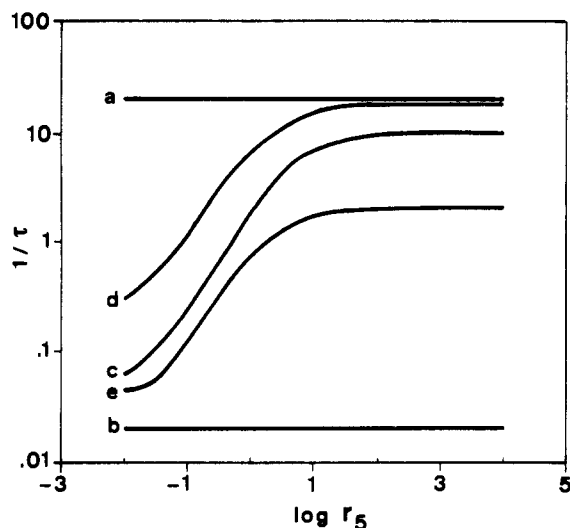


Figure 4. Change in probe orientational correlation time, τ , with the free-volume fluctuation rates, r_5 , of the matrix. The curves are drawn by using eq 27, with $r_1 = 0.01$ and $r_3 = 10$ for the cases (a) $p_s \rightarrow 0$, (b) $p_s \rightarrow 1$, (c) $p_s = 0.5$, (d) $p_s = 0.1$, and (e) $p_s = 0.9$. The t and c states are assumed to be equally probable in all cases.

with the elements of the following matrix

$$[f_{ij}] = [\mathbf{m}_i \cdot \mathbf{m}_j] = \begin{bmatrix} 1 & -1 & 1 & -1 \\ -1 & 1 & -1 & 1 \\ 1 & -1 & 1 & -1 \\ -1 & 1 & -1 & 1 \end{bmatrix} \quad (34)$$

Here \mathbf{m}_i refers to the vectorial representation of \mathbf{m} when bond BC is in state i . Substitution of eq 34 into eq 25 and the use of the latter in the right-hand side of eq 24 together with the eigenvalues given by eq 18 yield $M_1(t)$. The latter is particularly suitable for the description of dielectric relaxation, with the vector \mathbf{m} identifying the direction of the dipole moment under investigation.

Results of numerical calculations for the correlation time, τ , of the first OACF are shown in Figure 4 where τ^{-1} is presented as a function of the rate r_5 of the matrix for $r_1 = 0.01$ and $r_3 = 10$. r_5 is varied in the range $r_5 \geq r_1$ in accordance with the assumption of the model. The curves are obtained by using eq 27. Line a is obtained for the limit case where the matrix is in the fast state only, i.e., for $p_s \rightarrow 0$, while line b is representative of the other extreme case where $p_s \rightarrow 1$. Curves d, c, and e are drawn for the intermediate cases of $p_s = 0.1$, 0.5, and 0.9, respectively. In all cases, the t and c states are assumed to be equally probable in each matrix, thus leading to the equilibrium joint probabilities indicated in the figure caption. A smooth crossover from the slow to the fast regime is obtained for $1/\tau$ with an increasing rate r_5 of the matrix. In the slow regime $1/\tau$ increases with the mobility of the matrix, whereas in the fast regime, $1/\tau$ is independent of r_5 as indicated by the horizontal portions of the curves.

The fast and slow matrix approximations given by eqs 29 and 31 are compared in Figure 5 with the exact calculations from eq 27 for $r_1 = r_2 = 0.01$, $r_3 = r_4 = 10$, and $p_{st} = p_{sc} = p_{ft} = p_{fc} = 1/4$. The solid curve represents the exact results from eq 27. The dashed curve is for the slow matrix approximation from eq 31. The dot-dashed curve is for the fast matrix approximation from eq 29.

An alternate definition of the correlation time is given¹⁰ as

$$\tau = -(1 - k_1) / \sum k_i \lambda_i \quad (35)$$

Defined in this manner, τ represents the intersection of

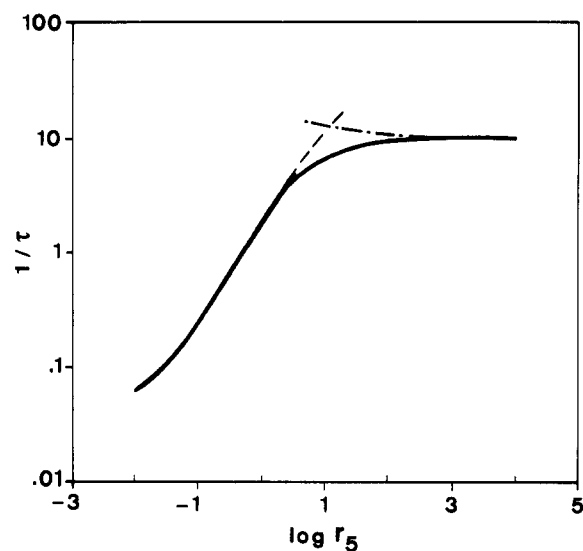


Figure 5. Dependence of τ on r_5 . The solid curve is identical with the curve c in Figure 4. The dashed and dot-dashed curves are obtained by using the approximate eqs 31 and 29 for the slow and fast regimes, respectively.

the initial tangent to the autocorrelation curve with its $t = \infty$ asymptote. If the relaxation process is a single-exponential decay process, the two definitions of τ given by eqs 26 and 35 are identical. For multiexponential decay, τ given by eq 35 emphasizes the faster modes of relaxation as follows from its definition. With reference to the model employed in the present study it is independent of the mobility of the environment. In fact, calculations show that for all values of r_5 it is equal to the upper limit of the correlation time predicted by eq 27. For this reason, this definition furnishes information on the probe intramolecular potential only.

Temperature Dependence. The observed activation energy, E_a , is defined as

$$E_a = -RT^2 \partial \ln(1/\tau) / \partial T \quad (36)$$

The latter reduces to simple mathematical expressions in the two limiting cases of fast and slow matrices, as presented below.

For fast matrices, eq 29 applies. Differentiation of the latter according to eq 36 after substitution of eq 9 for r_3 and r_4 yields

$$E_a = E_{tc} + RT^2 \partial \ln g_f / \partial T \quad (37)$$

assuming $r_3 \approx r_4$. Here $\partial \ln g_f / \partial T$ represents the temperature dependence of the free volume. It is given by

$$\partial \ln g_f / \partial T = \frac{A_1 A_2}{[A_2 + (T - T_0)]^2} \quad (38)$$

for media where linear dependence of v_f on T holds. Here the overbars on A_1 and A_2 , which were used in eqs 12 and 13, have been omitted inasmuch as the parameters in eq 38 correspond to the fast matrix. Alternately, the above temperature coefficient may be identified with the enthalpy change, ΔH_η , associated with the temperature dependence of the solvent viscosity, η . In cases where g_f approaches unity (i.e., a large free volume and/or high rate of fluctuations in the matrix), this term vanishes and the apparent activation energy equates to that of the intramolecular conformational transitions. In most cases, however, $\partial \ln g_f / \partial T$ is of comparable magnitude to the intramolecular potentials and the contribution of both terms in eq 37 is experimentally observed.^{1,2} In the case of *meso-*

2,4-di-*N*-carbazolypentane dispersed in isooctane, for instance, the apparent activation energy turns out to equate to the sum of the probe intramolecular conformational barrier (~ 2 kcal/mol) and the energy change of viscous origin (~ 2 kcal/mol).

In the other extreme case of very slow matrix, τ increases indefinitely as r_5 decreases, as indicated by eq 32. Thus, the temperature dependence of τ is necessarily the one dictated by the matrix only and the latter is deduced from eqs 10, 11, and 13 as

$$E_a = RT^2 \partial \ln g_s / \partial T \quad (39)$$

The observed WLF behavior for probes dispersed in bulk polymers is a common example for this situation.^{1,12}

Differentiation of the complete expression 27 according to eq 36 leads to a rather complicated expression for E_a in which the simple factorization of the apparent activation energy into an Arrhenius and a WLF term is not possible. Nevertheless, eq 27 can still be employed to derive the temperature dependence of the activation energy by numerical methods.

Conclusion

In the present study, a simple model is proposed to investigate the dynamics of internal conformational transitions coupled to environmental free-volume fluctuations. Accordingly, two states, fast and slow, are assigned to the environment as a first approximation to the more realistic case of a distribution of free volume. However, this approximation is particularly convenient for excimer-forming probes in which the excimer formation does not take place unless a sufficiently large threshold free volume allowing for the well-defined geometric rearrangement is provided by the environment.

A fundamental assumption underlying the theory is that the conformational transitions in a given molecule assume different rates depending on the nature, fast or slow, of its close intermolecular neighborhood while the reorientations or free-volume fluctuations in the neighborhood are not affected by the isomeric state of the molecule. The resulting kinetic scheme for the simple isomeric transition $t \rightleftharpoons c$ is portrayed in Figure 2.

In the mean-field approach adopted in previous work,⁹ the resistance of the environment to motion is implicitly considered only through the effective friction coefficient in the preexponential factor of the rate constants for intramolecular conformational transitions. Here a more realistic approach is undertaken: the local environment of the reorienting molecule or probe is allowed to fluctuate in time, thus giving rise to temporal increases or decreases of free volume which in turn modulates the rates of intramolecular rearrangements in the probe. Instead of a single relaxational mode representative of the $t \rightleftharpoons c$ transition of the probe in a mean-field approximation, now two distinct modes with frequencies $|\lambda_3|$ and $|\lambda_4|$ (eq 18), each including explicitly the joint effect of intramolecular energetics and local free-volume fluctuations, are operative.

The resulting correlation time as a function of the rate r_5 of free-volume fluctuations exhibits, as may be seen from Figures 4 and 5, a clear transition from the diffusion-controlled regime where τ decreases with increasing r_5 to the plateau region at large r_5 where τ becomes independent of r_5 . In this latter regime the general eq 27 is satisfactorily approximated by the simple expression 29, which is identical with the behavior predicted by a mean-field approach. For systems in that domain, the temperature dependence exhibits the additive contributions of that of

the mean friction coefficient and the intramolecular potential barrier. In the slow matrix regime, however, the confinement of probe transition rates r_1 and r_2 to values lower than or equal to the free-volume fluctuation rates, leads to eq 31 and ultimately eq 32 where the mobility of the matrix governs the dynamics of the probe. This explains the observed WLF type temperature dependence for probes dispersed in bulk polymers such as polybutadiene, poly(propylene oxide), polyisobutylene, ethylene-propylene copolymer, and polyisoprene.¹²

Acknowledgment. Financial support by NATO Grant 0321/87 is gratefully acknowledged. We thank Dr. L. Bokobza for stimulating discussions.

Appendix

Coupling of Longer Probes with the Matrix. Relaxation of the probe-matrix system where the probe and the matrix may have more than two states follows essentially the same arguments as presented in the preceding section. For a larger number of states, a numerical solution of the master equation is necessary.

The dynamics of a probe in which rotations are possible about more than a single bond is of interest. The analysis may be carried out in a manner similar to a recent treatment¹¹ of the single chain.

Let us assume that independent rotations about n bonds are possible in a chain. Let $\mathbf{A}^{(n)}$ denote the corresponding transition rate matrix. Its eigenvalues will be indicated as $\lambda^{(n)}$. For simplicity we assume again that each bond has two states and the matrix has two states. The matrix $\mathbf{A}^{(n)}$ may be written¹¹ in terms of $\mathbf{A}^{(n-1)}$ and \mathbf{A} as

$$\mathbf{A}^{(n)} = \mathbf{A} \otimes \mathbf{I}^{(n-1)} + \mathbf{I} \otimes \mathbf{A}^{(n-1)} \quad (\text{A1})$$

where \mathbf{I} is the fourth-order identity matrix, and $\mathbf{I}^{(n-1)}$ is the direct product \otimes of \mathbf{I} , $n-1$ times by itself. The characteristic equation of $\mathbf{A}^{(n)}$ is

$$\det [\mathbf{A}^{(n)} - \lambda^{(n)} \mathbf{I}^{(n)}] = \begin{vmatrix} \mathbf{D}_1 & r_2 \mathbf{I}^{(n-1)} & r_6 \mathbf{I}^{(n-1)} & 0 \\ r_1 \mathbf{I}^{(n-1)} & \mathbf{D}_2 & 0 & r_6 \mathbf{I}^{(n-1)} \\ r_5 \mathbf{I}^{(n-1)} & 0 & \mathbf{D}_3 & r_4 \mathbf{I}^{(n-1)} \\ 0 & r_5 \mathbf{I}^{(n-1)} & r_3 \mathbf{I}^{(n-1)} & \mathbf{D}_4 \end{vmatrix} = 0 \quad (\text{A2})$$

where \mathbf{D}_i ($i = 1-4$) are given by

$$\mathbf{D}_1 = \mathbf{A}^{(n-1)} - (\lambda^{(n)} + r_1 + r_5) \mathbf{I}^{(n-1)}$$

$$\mathbf{D}_2 = \mathbf{A}^{(n-1)} - (\lambda^{(n)} + r_2 + r_5) \mathbf{I}^{(n-1)}$$

$$\mathbf{D}_3 = \mathbf{A}^{(n-1)} - (\lambda^{(n)} + r_3 + r_6) \mathbf{I}^{(n-1)}$$

$$\mathbf{D}_4 = \mathbf{A}^{(n-1)} - (\lambda^{(n)} + r_4 + r_6) \mathbf{I}^{(n-1)}$$

Equation A2 may be rearranged to yield

$$\det [\mathbf{A}^{(n)} - \lambda^{(n)} \mathbf{I}^{(n)}] = \prod_{k=1}^4 \det [\mathbf{A}^{(n-1)} - (\lambda^{(n)} - \lambda_k) \mathbf{I}^{(n-1)}] \quad (\text{A3})$$

where λ_k is given by eq 18. Equation A3 leads to the recurrence equation

$$\lambda_i^{(n)} = \lambda_i^{(n-1)} + \lambda_k \quad k = 1-4 \quad (\text{A4})$$

where $\lambda_i^{(n)}$ ranges from $4^{n-1}(k-1) + 1$ to $4^{n-1}k$ for each k . Thus starting from the four eigenvalues representative of single bond motion, one can build the set of eigenvalues or relaxational frequencies characterizing the motion

of independent bonds. Also the corresponding eigenvectors and eigenrows may be evaluated by suitable combination of those given by eqs 20-23, in accordance with the formulation recently given.¹¹

References and Notes

- (1) Pajot-Augy, E.; Bokobza, L.; Monnerie, L.; Castellan, A.; Bouas-Laurent, H.; Millet, C. *Polymer* **1983**, *24*, 117. Bokobza, L.; Pajot-Augy, E.; Monnerie, L.; Castellan, A.; Bouas-Laurent, H. *Polym. Photochem.* **1984**, *5*, 191. Pajot-Augy, E.; Bokobza, L.; Monnerie, L.; Castellan, A.; Bouas-Laurent, H. *Macromolecules* **1984**, *17*, 1490. Pham-Van-Cang, C.; Bokobza, L.; Monnerie, L.; Vandendriessche, J.; De Schryver, F. C. *Polym. Commun.* **1986**, *27*, 89. Bokobza, L.; Monnerie, L. In *Photophysical and Photochemical Tools in Polymer Science*; Winnik, M. A., Ed.; D. Reidel: Dordrecht, The Netherlands, 1986. Bokobza, L.; Pham-Van-Cang, C.; Monnerie, L.; Vandendriessche, J.; De Schryver, F. C. *Polymer* **1989**, *30*, 45.
- (2) Vandendriessche, J.; Van der Auweraer, M.; De Schryver, F. C. *Bull. Soc. Chim. Belg.* **1985**, *94*, 991.
- (3) Glarum, S. H. *J. Chem. Phys.* **1960**, *33*, 639.
- (4) Anderson, J. E.; Ullman, R. *J. Chem. Phys.* **1967**, *47*, 2187.
- (5) Anderson, J. E. *J. Chem. Phys.* **1967**, *47*, 4879.
- (6) Sillescu, H. *J. Chem. Phys.* **1971**, *54*, 5.
- (7) Bahar, I.; Erman, B. *Macromolecules* **1987**, *20*, 1368. Bahar, I.; Erman, B.; Monnerie, L. *Macromolecules* **1989**, *22*, 2403.
- (8) Kramers, H. A. *Physica* **1940**, *7*, 284.
- (9) Doolittle, A. J. *Appl. Phys.* **1951**, *22*, 1471.
- (10) Schwarz, G. *Rev. Mod. Phys.* **1986**, *40*, 206.
- (11) Kloczkowski, A.; Mark, J. E.; Bahar, I.; Erman, B. *J. Chem. Phys.* **1990**, *92*, 4513.
- (12) See for example: Bokobza, L.; Pham-Van-Cang, C.; Giordano, C.; Monnerie, L.; Vandendriessche, J.; De Schryver, F. C. *Polymer* **1987**, *28*, 1876.

Monte Carlo Simulations of Linear and Cyclic Chains on Cubic and Quadratic Lattices

Johannes Reiter

Max-Planck-Institut für Polymerforschung, Postfach 3148, D-6500 Mainz, F.R.G.

Received October 6, 1989; Revised Manuscript Received February 2, 1990

ABSTRACT: A Monte Carlo algorithm for hypercubic lattices is investigated that combines end and kink reptations with local dynamic motions. It can be used for linear chains, for rings, and for the equilibration of the arms of star polymers. The algorithm fulfils the condition of detailed balance, and it is ergodic for a single linear chain. For the special case of a cyclic chain in two dimensions, a proof of ergodicity is also given. The statistical properties of the algorithm are discussed and, as examples, chain dimensions of linear and cyclic chains are computed.

Introduction

There are many algorithms known for the simulation of single macromolecules on a lattice.¹ Here we want to discuss yet another algorithm that might be used with advantage in some applications. The following motions are used: (1) inversion of L-structures, end turns, and (2) general reptation moves where a kink or end group is transported via a conformation change along the chain; see Figure 1. The latter motions include, as special cases, mere rotations of a kink, i.e., the well-known crankshaft motions, and reptations of the whole chain, i.e., slithering snake motions. Crankshaft motions combined with the inversion of L-structures and rotation of end segments are known not to be ergodic, and, in two dimensions, new bonds are generated only at the ends;¹ i.e., with these motions rings in two dimensions cannot be simulated. Because of the long-range transport of kinks, these disadvantages are avoided here. Long-range transport of kinks has already been used for dense systems at a volume fraction of unity in the collective motion algorithm.²⁻⁴ Long-range motions have also been used by Skolnick et al. in simulations of lattice models for protein.⁵ For single chains, removal and insertion of kinks has been introduced by Berg and Foerster⁶ and de Carvalho et al.^{7,8} in a grand canonical simulation of chains with varying length,^{1,9} and the statistical properties of that algorithm have been discussed by Caracciolo and Sokal.⁹ They demonstrated, for instance, that these motions are ergodic. As shown here

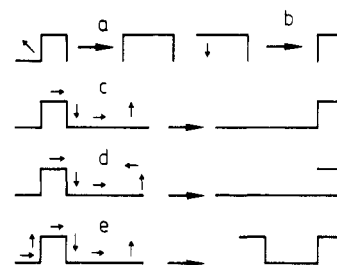


Figure 1. (a) L-inversion. (b) End turn. (c, d) General reptation motions are shown, where the chain changes conformation by a disappearance of a movable group, a slithering motion along the contour, and the formation of a movable group. (c) Kink-kink reptation. (d) Kink-end reptation. In the example shown, the end group takes on a kink conformation, but it could also take on other conformations. (e) End-kink reptation. Other motions not shown include end-end reptation, i.e., the familiar slithering snake motion, the rotation of a kink (crankshaft motion), and the conformation change of an end group containing two beads.

the removal and insertion of a kink (or an end group) can be combined into one step which is still ergodic.

The paper is organized as follows. First, the algorithm is discussed in detail and a proof for ergodicity for linear chains in any dimension and for cyclic chains in two dimensions is given. Then variants of the algorithm are discussed which might be used for denser systems. Finally, chain dimensions computed with the algorithm for linear